Observation of Electron Density Fluctuations by Using the O-Mode Microwave Imaging Reflectometry (O-MIR) in LHD*)

Yoshio NAGAYAMA[1,2], Soichiro YAMAGUCHI[3], Zongbing SHI[4], Hayato TSUCHIYA[1], Shigehiro HASHIMOTO[1], Naoki ITO[5], Min JIANG[3], Daisuke KUWAHARA[6] and Shoji SUGITO[7]

[1]*National Institute for Fusion Science, Toki 509-5292, Japan*
[2]*The Graduate University for Advanced Studies, Toki 509-5292, Japan*
[3]*Kansai University, Suita 564-8680, Japan*
[4]*Southwestern Institute of Physics, Chengdu 610041, China*
[5]*National Institute of Technology, Ube College, Ube 755-8555, Japan*
[6]*Tokyo University of Agriculture and Technology, Koganei 184-8588, Japan*
[7]*The Institute for Molecular Science, Okazaki 444-8585, Japan*

(Received 30 November 2015 / Accepted 16 June 2016)

The O-mode microwave imaging reflectometry (O-MIR) has been developed. The frequency is 26 - 34 GHz, which corresponds to the cutoff electron density of $0.8 - 1.5 \times 10^{19}\,\mathrm{m}^{-3}$. Since the local wave of the newly developed horn antenna millimeter wave imaging device (HMID) is fed by coaxial cable, the optical system of O-MIR is significantly simplified. By using O-MIR, the edge electron density fluctuation in an H-mode plasma is observed in LHD. The spectrum in the wave number and the frequency (k - ω) space is obtained by using the two-point correlation analysis. In the H-mode plasma the fluctuation amplitude is higher and the k - ω spectrum has the feature of the drift wave.

Keywords: microwave, imaging, reflectometry, diagnostics, plasma, LHD, helical, electron density, fluctuation

DOI: 10.1585/pfr.11.2402111

1. Introduction

It is considered that thermal conduction and particle diffusion are governed by turbulences. Turbulences are generated by the micro instabilities, which are accompanied by the electron density fluctuations. Visualization of local electron density fluctuations will be very useful to study the physics of confinement and instabilities in fusion plasma. Plasma reflects the O-mode microwave at the cutoff frequencies, that is,

$$\frac{\omega_{\mathrm{pe}}}{2\pi}[\mathrm{GHz}] = 28.4\sqrt{n_{\mathrm{e}}\,[10^{19}\,\mathrm{m}^{-3}]}. \quad (1)$$

This is the reason why the microwave imaging reflectometry (MIR) will be one of the most powerful diagnostics of local electron density fluctuations [1].

In the Large Helical Device (LHD), MIR has been intensively developed [2–9]. The X-mode MIR system had been used to date [10]. Usually, the electron density profile is hollow in an LHD plasma, thus the X-mode reflectometry is useful for observing the plasma center because the cutoff frequency is a function of both the electron density and the magnetic field. However, observable plasma is very limited. For example, the setting frequency of X-MIR is too low to observe the ion internal transport barrier (ITB) in LHD. Since the electron density profile is peaked in the ion ITB plasma, the O-mode MIR (O-MIR) is useful for observing the ITB region. Usually, the electron density is $1 - 1.5 \times 10^{19}\,\mathrm{m}^{-3}$ in the ITB region in LHD, and the cutoff frequency of the O-mode wave is 28 - 35 GHz from eq. (1). In this paper, we will present the O-MIR system and the electron density fluctuations in the H-mode plasma in LHD.

2. O-MIR System

The schematic diagram of the O-MIR imaging optics is shown in Fig. 1. In O-MIR, four frequencies between 26 and 35 GHz simultaneously illuminate the LHD plasma. Thus, the observable density is $0.8 - 1.5 \times 10^{19}\,\mathrm{m}^{-3}$. The O-MIR system has 8 poloidal channels, 8 toroidal channels, and 4 radial channels.

A wave synthesizer, which is controlled by a computer with a LabVIEW program, generates the local oscillation (LO) wave (f_{LO}). Four voltage controlled oscillators generate different frequencies (f_{RFj}). The reference frequency (f_{ref}) is generated by a crystal oscillator. By using up-converters, all of those frequencies are mixed. Since the synthesizer can generate up to 10 GHz, frequencies are multiplied by the use of × 4 frequency multipliers, as $\omega_{\mathrm{LO}}/2\pi = 4 \times f_{\mathrm{LO}}$, $\omega_{\mathrm{j}}/2\pi = 4 \times f_{\mathrm{RFj}}$, and $\omega_{\mathrm{r}}/2\pi = 4 \times f_{\mathrm{ref}}$. The final frequencies are as follows: $\omega_{\mathrm{LO}}/2\pi =$

author's e-mail: nagayama.yoshio@nifs.ac.jp
*) This article is based on the presentation at the 25th International Toki Conference (ITC25).

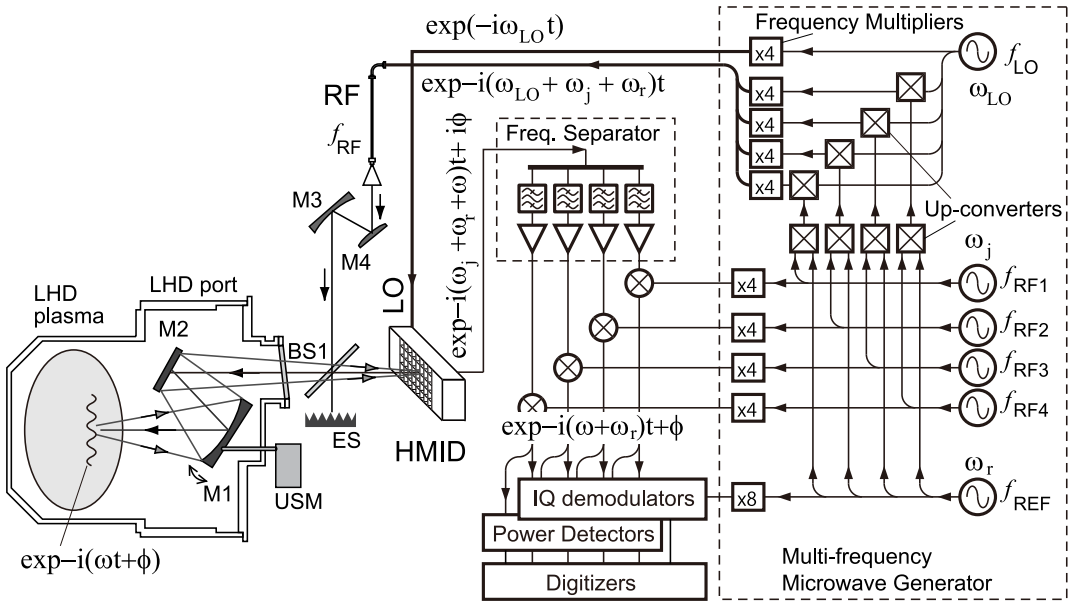

Fig. 1 Schematic diagram of the O-mode microwave imaging reflectometry (O-MIR) system in LHD.

22 - 26 GHz, $\omega_j/2\pi$ = 4.5, 5.9, 7.1, 8.7 GHz, and $\omega_r/2\pi$ = 110 MHz. The actual illumination frequency (ω_{RF}) is ω_{RF} = ω_{LO} + ω_j+ω_r.

The illumination wave is radiated by a Ka-band rectangular horn antenna and is expanded by mirrors (M_3, M_4) in order for the parallel beam to illuminate the plasma. The plasma reflects the illumination wave on the reflection layer with the cutoff density corresponding to the illumination frequency. The reflected wave is modulated by the fluctuation (ω, ϕ) of the reflection surface [11]. Since the reflection surface is not smooth or flat, the microwave is scattered on the reflection surface.

The plasma image of the scattered wave is detected by the Horn-antenna Millimeter Imaging Device (HMID), which is newly developed based upon the new concept [12]. The 2D HMID in LHD is made as eight stacked 1D HMID pieces, and each 1D HMID has 8ch. In the 1D HMID, a printed circuit board (PCB) is installed between aluminum frames, each of which have the half cut horn antenna array. The signal wave (ω_{RF}) entering into the horn antenna is transduced to the micro-strip line by the fine-line transducer. The signal wave is amplified by an RF amplifier before mixing in order to compensate the conversion loss of the double balanced mixer (DBM). The local oscillation (LO) wave (ω_{LO}) is delivered to each 1D HMID by coaxial cables, and is divided by the Wilkinson power divider on the PCB of the 1D HMID. The LO optics which were required in the X-MIR [10] are not required, thus the imaging optics become significantly simplified in the O-MIR. In the DBM, the RF wave and the LO wave are mixed, and the intermediate frequency (IF) signal (ω_{IF} = ω_j+ ω_r) is generated.

In the frequency separator, the IF signals are separated into four frequencies by BPFs. Also, they are mixed with ω_j from the VCO in the frequency separator, thus all signals become the same frequency (ω_r = 110 MHz). Each signal thus is amplified by a narrow band amplifier with the central frequency of ω_r and the phase is detected by the quadrature (I-Q) demodulator, of which the reference signal comes from the crystal oscillator. The power is detected by the linear scale power detector so that the small fluctuations can be easily distinguished. Typical fluctuation level is 10 times higher than the noise level in the output of the power detector.

3. Experiment

By using the O-MIR we observe the edge density fluctuation in the H-mode plasma. Figure 2 shows time evolution of averaged beta and H_α line emission, and radial profiles of the electron density and temperature in the H-mode plasma. Sudden drop of H_α line emission and the increment of beta at t = 3.788 sec indicate the H-mode transition. In this shot, $\omega_{LO}/2\pi$ = 25.5 GHz.

Key parameters of fluctuation are the wave number (k) and the frequency (ω). In this paper, in order to obtain the $k - \omega$ spectrum, we use the two-point cross-spectrum (S_{ij} (ω)) [13–16], which is defined as

$$S_{ij}(\omega) = \left\langle F_i^*(\omega) F_j(\omega) \right\rangle, \tag{2}$$

where the asterisk (*) and the brackets ($\langle\rangle$) denote the complex conjugate and the ensemble averaging, respectively. $F_j(\omega)$ is the Fourier transform of the MIR signal (f_j (t)) of the j-th channel. The wave-number (k_{ij}) between two MIR channels (i, j), of which distance is d_{ij}, can be obtained as

$$k_{ij} = \frac{1}{d_{ij}} \tan^{-1}\left(\frac{\mathrm{Im}S_{ij}(\omega)}{\mathrm{Re}S_{ij}(\omega)}\right). \tag{3}$$

The group velocity of the fluctuation (v_g) is obtained as

$$v_g = \frac{\mathrm{d}\omega}{\mathrm{d}k}. \tag{4}$$

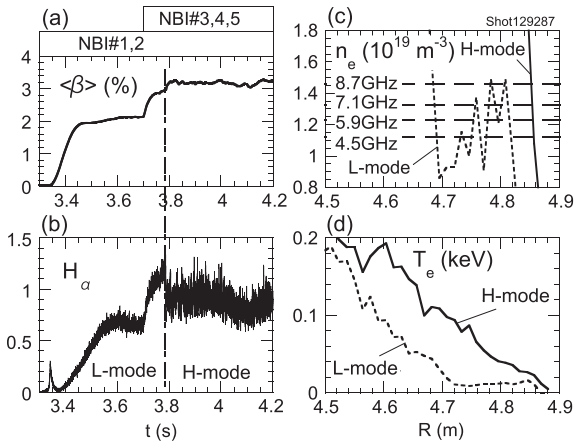

Fig. 2 (a) Time evolution of averaged beta; (b) H_α line emission. (c) The electron density profile and the cutoff densities corresponding to IF frequencies; (d) The electron temperature profile. Dotted line indicates L-mode (t = 3.6 - 3.7 sec) and the solid line H-mode (t = 3.9 - 4 sec).

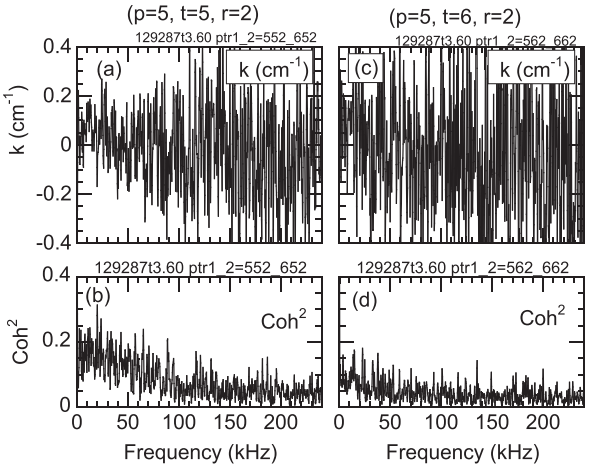

Fig. 3 (a) (c) Poloidal wave number of the edge density fluctuation in the L-mode plasma at the two positions, which are separated by 2.2 cm in toroidal (t) directions; (b) (d) Squared coherence corresponding to (a) and (c).

The coherence ($\mathrm{coh}_{ij}(\omega)$) is the normalized cross-power spectrum, as

$$\mathrm{coh}^2_{ij}(\omega) = \frac{\left|S_{ij}(\omega)\right|^2}{S_{ii}(\omega)S_{jj}(\omega)}. \quad (5)$$

The coherence indicates the reliability of the spectrum.

Figures 3 and 4 show typical examples of the poloidal wave number and the squared coherence of the L-mode plasma and the H-mode plasma, respectively. The wave number and the coherence are obtained between two neighboring channels in the poloidal direction. The imaging optics expands the HMID image to the plasma at R = 4.8 m by 1.1. Since the channel separation of HMID is 2 cm, the frames in Figs. 3 and 4 are separated by d_{ij} = 2.2 cm. Here, p indicates the relative poloidal position.

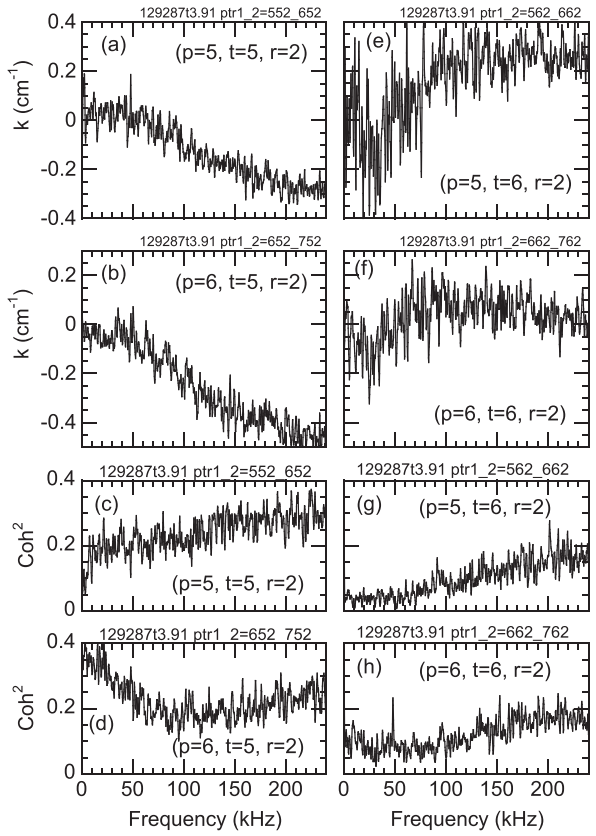

Fig. 4 (a) (b) (e) (f) Poloidal wave number of the edge density fluctuation in the H-mode plasma at the 4 positions, which are separated by 2.2 cm in poloidal (p) and toroidal (t) directions; (c) (d) (g) (h) Squared coherence corresponding to (a), (b), (e) and (f).

The frequency of the MIR illumination wave is $\omega_j/2\pi$ = 5.9 GHz. The reflection position can be seen as the cross section of the electron density profile and the cutoff density for 5.9 GHz in Fig. 2 (c). The radial position of the fluctuation is very close to the plasma boundary in both cases of L-mode and H-mode. The theoretical calculation of field lines indicates that the last closed flux surface (LCFS) in the vacuum is at R = 4.45 m. So, the observed region is in the stochastic region in the vacuum field.

The k_p - ω curve in Figs. 3 and 4 may represent the dispersion relation of density fluctuation at the plasma edge. In the case of L-mode, the fluctuation signal is more than 3 times higher than the noise level, but the coherence is as low as noise level and the k_p - ω curve is not clear. As shown in Fig. 2 (c), the electron density profile is not clear in the observed region (R = 4.7 - 4.8 m). The electron temperature is very low (50 eV) and the profile is flat. The pressure may be so low that the fluctuation level is low in this region.

In the cases of H-mode, the observed region is localized near R = 4.85 m, where the density gradient is steep (Fig. 2 (c)), and the temperature profile is not flat (Fig. 2 (d)). Thus, the plasma confinement structure is different from the L-mode.

In the toroidal section noted by $t = 5$, the k_p - ω curve is linear. This is a feature of the drift wave. The group velocity of the fluctuation is -3.2×10^4 m/sec and -2.1×10^4 m/sec in the case of Figs. 4 (a) and 4 (b), respectively. Here positive sign in the velocity indicates the direction of the electron diamagnetic drift motion in our experimental set-up. At the observation point ($R = 4.85$ m) the phase velocity of the drift wave ($v_{ph} = \omega_{*e}/k$) is 750 m/sec, where ω_{*e} is the electron diamagnetic frequency that is defined as

$$\omega_{*e} = -k\frac{T_e}{eB}\frac{dn}{ndr}. \quad (6)$$

The observed velocity is much faster than the drift wave. In the LHD edge plasma, the electrostatic potential is positive because the electrons tend to escape along the open field line [17]. Therefore, the velocity may be due to the $E \times B$ rotation.

Interestingly, the k_p - ω curve is different at the different toroidal positions. In the neighbor toroidal section that is noted by $t = 6$, the k_p - ω curve between 30 and 100 kHz is bent in the opposite direction as shown in Figs. 4 (e, f). The group velocity of the fluctuation between 30 and 100 kHz is 1.2×10^4 m/sec and 1.5×10^4 m/sec in the case of Fig. 4 (e) and Fig. 4 (f), respectively.

4. Conclusion

The O-mode MIR system and the 30 GHz HMID have been newly developed. Many technologies, such as fin-line transducer, RF amplifier and DBM, which are used for HMID, and the optimization of LO power improve the MIR sensitivity significantly. By using O-MIR, electron density fluctuations are measured at the H-mode edge in LHD. The k_p - ω curves are obtained by the two-point correlation analysis. Basically, this is linear like a drift wave. However, the group velocity is much faster than the theoretical phase velocity of the drift wave. The group velocity is different at the different positions. Furthermore, the direction of poloidal phase velocity of the fluctuation is different at the different toroidal positions. Further research is required to understand these phenomena.

Acknowledgments

This work is supported by NIFS/NINS under the project of Formation of International Scientific Base and Network (No. KEIN1111) and by NIFS LHD project (No. ULPP008), and by KAKENHI (No. 15K12564). This work is technically supported by the Equipment Development Center, Institute for Molecular Science.

[1] E. Mazzucato, Nucl. Fusion **41**, 203 (2001).
[2] S. Yamaguchi, Y. Nagayama, R. Pavlichenko, S. Inagaki, Y. Kogi and A. Mase, Rev. Sci. Instrum. **77**, 10E930 (2006).
[3] S. Yamaguchi, Y. Nagayama, Z. Shi, R. Pavlichenko, S. Inagaki *et al.*, Plasma Fusion Res. **2**, S1038 (2007).
[4] S. Yamaguchi, Y. Nagayama, D. Kuwahara, T. Yoshinaga, Z.B. Shi *et al.*, Rev. Sci. Instrum. **79**, 10F111 (2008).
[5] D. Kuwahara, S. Tsuji-Iio, Y. Nagayama, T. Yoshinaga, Z. Shi *et al.*, J. Plasma Fusion Res. SERIES **8**, 649 (2009).
[6] D. Kuwahara, S. Tsuji-Iio, Y. Nagayama, T. Yoshinaga, Z. Shi *et al.*, J. Plasma Fusion Res. SERIES **9**, 125 (2010).
[7] D. Kuwahara, S. Tsuji-Iio, Y. Nagayama, T. Yoshinaga, H. Tsuchiya *et al.*, Rev. Sci. Instrum. **81**, 10D919 (2010).
[8] T. Yoshinaga, Y. Nagayama, D. Kuwahara, H. Tsuchiya *et al.*, Rev. Sci. Instrum. **81**, 10D915 (2010).
[9] T. Yoshinaga, D. Kuwahara, Y. Nagayama, H. Tsuchiya, S. Yamaguchi *et al.*, Plasma Fusion Res. **5**, 030 (2010).
[10] Y. Nagayama, D. Kuwahara, T. Yoshinaga, Y. Hamada, Y. Kogi *et al.*, Rev. Sci. Instrum. **83**, 10E305 (2012).
[11] Z. Shi, Y. Nagayama, D. Kuwahara, T. Yoshinaga, M. Sugito *et al.*, J. Plasma Fusion Res. SERIES **8**, 0109 (2009).
[12] D. Kuwahara, N. Ito, Y. Nagayama, T. Yoshinaga, S. Yamaguchi *et al.*, Rev. Sci. Instrum. **85**, 11D805 (2014).
[13] Z.B. Shi, Y. Nagayama, S. Yamaguchi, Y. Hamada and Y. Hirano, Plasma Fusion Res. **3**, S1045 (2008).
[14] Z.B. Shi, Y. Nagayama, S. Yamaguchi, D. Kuwahara, T. Yoshinaga *et al.*, Plasma Fusion Res. **5**, S1019 (2010).
[15] Z.B. Shi, Y. Nagayama, S. Yamaguchi, T. Yoshinaga, D. Kuwahara *et al.*, J. Plasma Fusion Res. SERIES **9**, 054 (2010).
[16] Z.B. Shi, Y. Nagayama, S. Yamaguchi, D. Kuwahara, T. Yoshinaga *et al.*, Phys. Plasmas **18**, 102315 (2011).
[17] K. Kamiya, K. Ida, M. Yoshinuma, C. Suzuki, Y. Suzuki *et al.*, Nucl. Fusion **53**, 013003 (2013).